Rafał Kozubski, Mirosław Kozłowski
M. Smoluchowski Institute of Physics,
Jagiellonian University
Kraków

ATOMIC MIGRATION AND ORDERING IN HIGH-TEMPERATURE INTERMETALLICS

Key words

intermetallics, atomic migration, chemical ordering kinetics, resistometry, Monte Carlo simulation

Abstract

Resistometric studies of "order-order" kinetics in NiAl (B2), Ni_3Al ($L1_2$), FePd ($L1_0$) and FePt ($L1_0$) intermetallics revealed multi-time-scale character of the relaxations in Ni_3Al, FePd and FePt and surprisingly low rate of the process in NiAl – known of a giant vacancy concentration. Corresponding simulation studies elucidated atomistics of the processes pointing at their relationship to diffusion. Simulations of the phenomena in FePt nano-films indicated an important effect of surfaces on the mechanism of structural transformations and reproduced the phenomenon of spontaneous $L1_0$-superstructure reorientation.

Streszczenie

Badania rezystometryczne kinetyki procesów "porządek-porządek" w układach NiAl (B2), Ni_3Al ($L1_2$), FePd ($L1_0$) and FePt ($L1_0$) wykazały w trzech ostatnich przypadkach współistnienie różnych skal czasowych w obserwowanych relaksacjach. Relaksacje w układzie NiAl o "gigantycznej" koncentracji wakancji okazały się zaskakująco wolne. Metodą symulacji komputerowych wyjaśniono "atomistyczne" przyczyny powyższych efektów oraz ich związki z dyfuzją. Symulacje analogicznych procesów w nano-warstwach układu FePt wykazały silny wpływ powierzchni na przebieg zjawisk oraz odtworzyły zjawisko spontanicznej reorientacji wariantów nadstruktury $L1_0$.

1. Introduction

High superstructure stability in a number of technologically attractive intermetallic compounds causes that "order-disorder" transitions in those materials occur at very high temperatures; in many cases the state of chemical long-range order is maintained up to the melting point. Small temperature variations of the degree η of long-range order (LRO) – i.e. of the concentration of antisite defects, is, however, experimentally observable in such systems in so-called "order-order" relaxation processes occurring after a sudden change of temperature within the domain of LRO [1]. Due to the high degree of long-range order the phenomena are controlled by atomic migration in almost perfect superstructure, whose predominating mechanism consists of specifically

correlated elementary jumps to nearest-neighbouring (nn) vacancies. There is an extended bibliography devoted to atomistic models of *diffusion* in long-range ordered systems. It has been known for decades that because elementary atomic jumps usually disturb LRO and thus are energetically costly, atoms migrate either by executing sequences of correlated atomic jumps effectively lowering the net migration energy, or by taking advantage of thermally or mechanically generated imperfections of LRO (see e.g. [1-3] and the references therein). It is important to realise that although both diffusion and "order-order" relaxations proceed due to the same atomic jumps, the situation in the latter is totally different. As a system now relaxes to a new equilibrium atomic configuration the constraints imposed upon atomic jumps disturbing LRO are no longer valid, which consequently leads to specific atomic jump correlation – different from that observed e.g. in standard diffusion processes occurring at constant degree of LRO. Two aspects of the monitored "order-order" kinetics are usually analysed: (i) structure of the relaxations (e.g. possible different time scales involved), (ii) the value of the activation energy $E_A^{(O-O)}$ and its relation to the activation energy $E_A^{(D)}$ for self-diffusion in the same system. Hence, the investigation provides an information on atomic dynamics, which is complementary to the one yielded by *steady-state* diffusion studies. On the other hand, it leads to understanding the atomistic mechanisms of the generation/destruction of chemical order in multicomponent crystals.

Extended studies of "order-order" kinetics carried out for the last decade covered the phenomena occurring in high-temperature

intermetallics ordered in different superstructures and aimed at the recognition of the effect of superlattice geometry on the process. The research strategy was focused on the elucidation of experimental results by means of atomistic simulations revealing specific atomic-jump statistics responsible for the details of observed kinetics.

2. Experimental studies

2.1. Examined systems

An "order-order" relaxation in a system almost perfectly long-range ordered up to the melting point was for the first time directly observed by means of resistometry in the $L1_2$-ordered Ni_3Al intermetallic compound [4]. The results of the subsequent extended experimental studies have been reviewed several years ago [1]. An interpretation of the results and their reference to diffusion data were feasible due to very good homogeneity of the Ni_3Al superstructure and low density of defects (as indicated by thorough TEM examination). The favourable conditions were mostly due to Ni_3Al which is a compound solidifying directly as a long-range ordered phase and, therefore, showing very low density of antiphase domain boundaries. Consequently, systems showing the highest possible stabilities of superstructures were chosen for further studies.

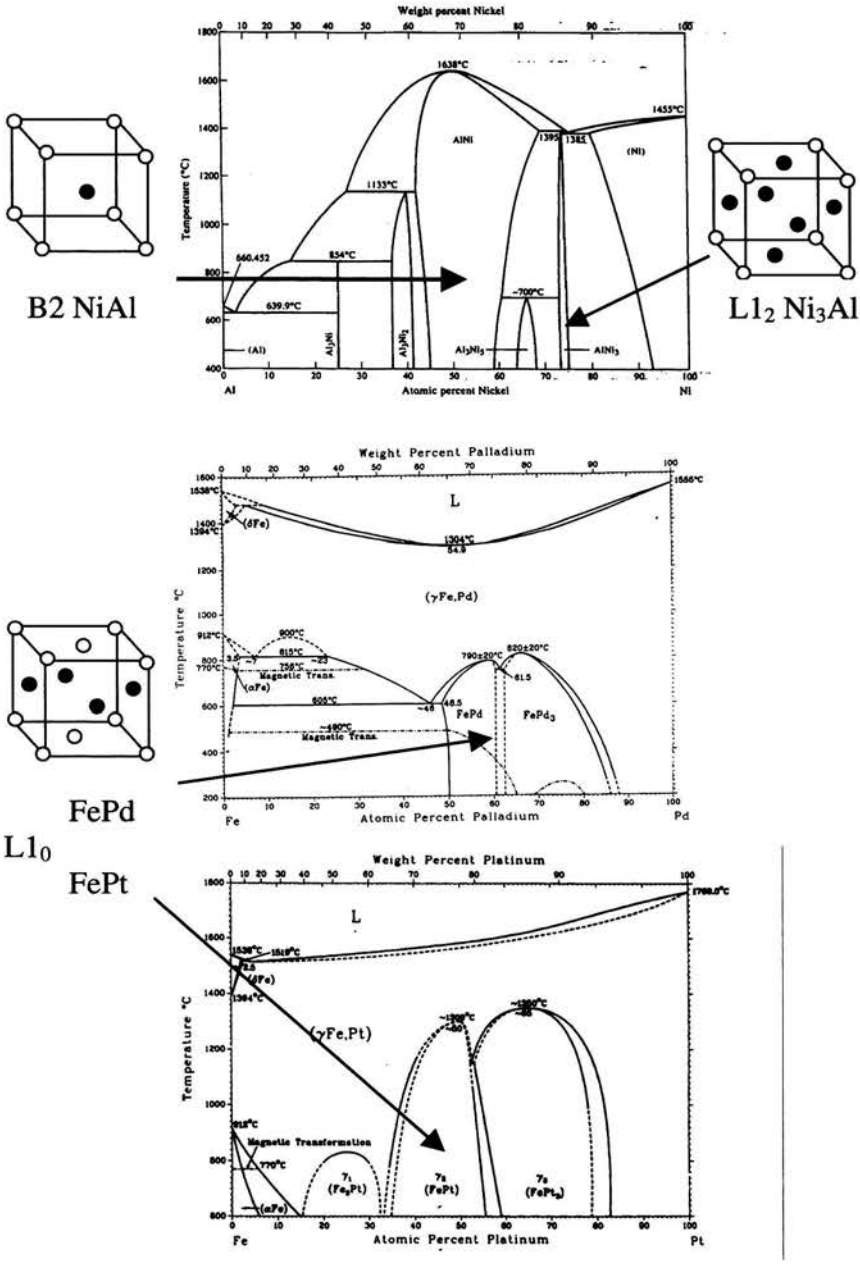

Fig.1. Phase diagrams [29] and superstructure schemes of the investigated intermetallic systems

The phase diagrams of the examined intermetallic systems representing three types of cubic (B2, $L1_2$) or tetragonal ($L1_0$) superstructures are reproduced in Fig. 1. While the samples of Ni_3Al, FePd and FePt were coarse-grained polycrystals, NiAl was a single crystal kindly supplied by Professor Alan J. Ardell, University of California, Los Angeles.

2.2. Experimental methods

The main experiments consisted of the following cycles of actions:

- Equilibration of the degree of LRO by annealing the sample at given temperature T_i ,
- Abrupt change of the annealing temperature to T_f ,
- Observation of the "order-order" relaxation in the sample at T_f,
- Subsequent change of annealing temperature to the new one T_f' once the relaxation at T_f shows saturation.

The low density of structural defects in the examined intermetallics was achieved at the expense of the amplitudes of measured "order-order" relaxations. This was required for two reasons: (i) for relaxation rates to be measurable (i.e. not too fast) the temperatures had to be well below the melting point; (ii) temperature steps $\Delta T = T_f - T_i$ had to be kept small enough so that the interpretation of the kinetics in terms of linearised equations is justified [5].

Effectively, the η amplitudes within "order-order" relaxations measured at $|\Delta T| \leq 50$ K never exceeded 0.5 % and this definitely

excluded diffraction techniques as experimental methods. Consequently, all the measurements were performed by means of resistometry.

The small amplitudes of "order-order" relaxations justify the assumption of proportionality between the observed changes of electrical resistivity and the corresponding changes of the degree of LRO. Both "in situ" and "residual resistometry (REST)" techniques were used; in each case the electrical resistivity was measured by means of the classical 4-point method with platinum electrodes point-welded to the sample positioned in a quartz tube filled with 5N Ar under slight overpressure. "In situ" measurements were carried out using a fully automated set-up with a mobile resistance furnace whose temperature was stabilised better than 1 K.

Quasi-residual resistometry (REST) experiments were carried out by means of a compact annealing-quenching line making it possible to perform series of annealings broken by quenching the sample in liquid nitrogen and measuring its electrical resistance without its re-installation in a resistometric holder.

2.3. Experimental results

A characteristics of the "order-order" relaxations in systems with fcc-based superstructures – i.e. in $L1_2$-ordered Ni_3Al [1] and in $L1_0$-ordered FePd [6,7] and FePt, is the observation of two different time

scales – an effect originally reported by Sitaud et al. [8][1]. The measured relaxations of electrical resistance R never fitted single exponentials, but a weighted sum of two exponentials with substantially different relaxation times:

$$\frac{R(t)-R_{EQ}}{R(t=0)-R_{EQ}} \approx C\cdot\exp\left(-\frac{t}{\tau_s}\right)+(1-C)\cdot\exp\left(-\frac{t}{\tau_l}\right); \qquad \tau_l > \tau_s; \quad 0\le C\le 1 \tag{1}$$

where: R_{EQ} denotes the asymptotically attained equilibrium value of R, t denotes time, τ_S and τ_l denote two different relaxation times and C denotes a weight factor showing the contribution of the fast component to the entire relaxation.

Since the effect occurred in up-step and down-step relaxations, the simplest explanation for the fast component, the elimination of excess vacancies, had to be excluded. The evaluated relaxation times showed linear Arrhenius plots (Figs.2 a, b) yielding activation energies marked on the raphs.

[1] *REST examination of FePd revealed two counteracting processes in „order-order" relaxations [6].*

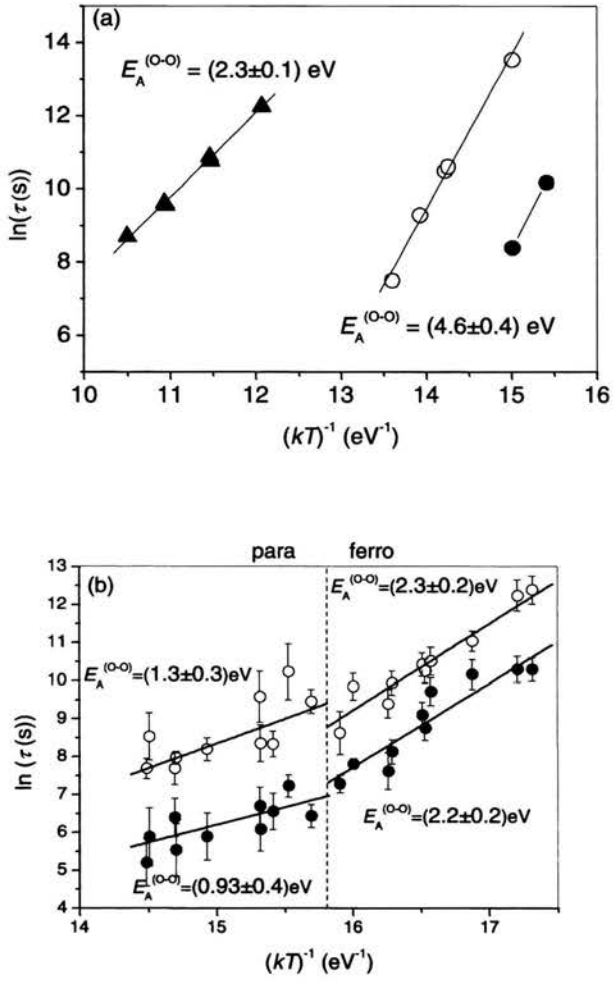

Fig.2. Arrhenius plots of the relaxation times τ for „order-order" kinetics evaluated from resistometric examinations: (a) Ni_3Al: fast process (●) and slow process (○), NiAl (▲); (b) FePd: fast process (●) and slow process (○) below and above the Curie point marked by a dashed line. Solid lines represent linear fits

In the case of FePd, the temperature range of the resistometric examination contained the Curie point T_C of the system. It follows from Fig.2b, that the activation energies of both (fast and slow) components of the relaxations registered "in situ" were markedly higher at temperatures below T_C. A similar effect was reported some years ago for the case of $L1_2$-ordered $Ni_3Al_{0,4}Fe_{0,6}$ [9].

The investigations of FePt are still in progress. The results show the coexistence of several different processes with different activation energies. The value of $E_A^{(O-O)}$=0,8 eV was obtained from a complete series of "in situ" resistometric measurements.

The evaluated activation energies $E_A^{(O-O)}$ of the "order-order" kinetics have been compared with the $E_A^{(D)}$ ones measured by tracer diffusion in the same systems. While $E_A^{(O-O)}$= 4,6 eV was higher than $E_A^{(D)}$= 3,0 eV [10] in $L1_2$-ordered Ni_3Al, such a relationship was not confirmed in cases of $L1_0$-ordered FePd ($E_A^{(D)}$= 2,6 eV [11]) and FePt ($E_A^{(D)}$= 2,9÷3,4 eV [12,13]) and rather seemed to be even inverted.

Binary phases with bcc-based B2 superstructure were represented by two systems: FeAl and NiAl. "Order-order" kinetics in FeAl appeared very complex and controlled by different mechanisms in particular temperature regions [14]. A more regular process was observed in NiAl [15]. However, the "order-order" relaxations showed extremely low rates. This becomes evident when Arrhenius plots of the "order-order" relaxation times of the examined Ni-Al intermetallics (Fig.2a) are compared. The plot corresponding to B2-ordered NiAl is shifted by about

200 K up in temperature compared to the one corresponding to Ni_3Al. This result was surprising in view of the enormous vacancy concentration C_V in NiAl, especially compared to Ni_3Al: $C_V = 1{,}4 \times 10^{-9}$ in Ni_3Al, $C_V = 7 \times 10^{-4}$ in NiAl. Both concentrations correspond to $T = T_M/2$, where T_M denotes the melting point [16]. Though being very sluggish, the "order-order" relaxations in NiAl showed a relatively low activation energy: $E_A^{(O-O)}$=2.3 eV; in view of $E_A^{(D)}$ = 3 eV for Ni-tracer in NiAl [17].

3. Computer simulations

3.1. Applied algorithms and implemented models

Dynamic Monte Carlo simulations appeared to be an efficient tool elucidating the basic features of "order-order" relaxations in intermetallics. The detailed atomistic image of the process elaborated some years ago for the case of $L1_2$-ordered Ni_3Al [18, 19] has now been extended to $L1_0$-ordered FePt.

The "order-order" kinetics was simulated by means of the Glauber algorithm implemented with vacancy mechanism of atomic jumps. The sample contained 40^3 $L1_2$ or $L1_0$ cells with lattice sites occupied by A and B atoms in stoichiometric proportion: A_3B for $L1_2$ and AB for $L1_0$ and a single vacancy (10 vacancies in [18]) was introduced to the system by emptying at random one lattice site. Periodic boundary conditions were imposed upon the sample.

The thin layers limited by free surfaces were modelled from the original bulk sample by removing periodic boundary conditions in the [001] direction, whereas the periodic boundary conditions were retained in [100]- and [010]-directions [20]. While the number of atomic layers in [001]-direction was reduced, the [100]- and [010]-sizes of the sample were increased, so that the total number of atoms is conserved. Initially, A and B atoms were distributed over the lattice sites in a perfect $L1_0$-type LRO. Two $L1_0$ variants were simulated:

- z-variant: with (001)-type monoatomic layers,
- x-variant: with (100)-type monoatomic layers.

A single MC step taken as a time unit consisted of a random choice of an atom from the first co-ordination shell of the vacancy and an attempt of its jump to the vacancy with the probability given by:

$$\Pi_{i\to j} = \frac{\exp\left[-\frac{\Delta E}{kT}\right]}{1+\exp\left[-\frac{\Delta E}{kT}\right]} \tag{2}$$

where:

i and j denote the initial positions of the atom and vacancy, respectively,

ΔE is the change of system energy due to the jump,

k and T are Boltzmann constant and absolute temperature, respectively.

ΔE was calculated within the pair approximation with atomic interactions $V_{\text{i-k}}$ in two co-ordination shells. The parameters $V_{\text{i-k}}$ were evaluated with reference to experimental and theoretical data of Ni_3Al and FePt: diffuse scattering experiments and "embedded atom" (EAM) potentials for Ni_3Al

[18,19] and "ab initio" calculations combined with Cluster Expansion (CE) for FePt [21]. No interaction with and between vacancies was assumed.

The following parameters were monitored as functions of the number of MC steps:

(i) Bragg-Williams-type LRO parameter η

$$\eta = 1 - \frac{N_A^{(B)}}{c_A \times N^{(B)}}, \tag{3}$$

where:

$N_A^{(B)}$ denotes the number of A-antisite atoms

$N^{(B)}$ denotes the number of B-sublattice sites

c_A denotes A-atom concentration

(ii) short-range order (SRO) parameter *APC* (Antisite-Pair-Correlation):

$$APC = \frac{N_{AB}^{(B)(A)}}{N_A^{(B)}}, \tag{4}$$

where: $N_{AB}^{(B)(A)}$ denotes the number of nn pairs of A- and B-antisite atoms.

(iii) SRO parameters *NNCOR* used when simulating nano-layers defined as:

$$NNCOR_{\mathrm{Fe}} = \frac{2 \times N(\mathrm{Fe}\ \ nn\ \ \mathrm{Fe})}{N_{\mathrm{Fe}}} \quad \text{and}$$

$$NNCOR_{\mathrm{Pt}} = \frac{2 \times N(\mathrm{Pt}\ \ nn\ \ \mathrm{Pt})}{N_{\mathrm{Pt}}} \tag{5}$$

where N(Fe *nn* Fe) or N(Pt *nn* Pt) are the numbers of Pt-Pt or Fe-Fe nn pairs in the system and N_{Pt} and N_{Fe} denote the numbers of Pt and Fe atoms, respectively.

(iv) "jump-frequency" parameters $P_{A:i \to j}$:

$$P_{A:i \to j} = \frac{N_{A:i \to j}}{N_{att}}, \tag{6}$$

where $N_{\mathrm{A:i} \to \mathrm{j}}$ denotes the number of A-atom jumps from positions "*i*" to nn vacancies residing in positions "*j*" within a fixed number of MC steps; N_{att} denotes the number of all jump attempts within the same time period.

All the simulations discussed in the present paper were performed in a way that the initial state of the sample corresponded to $T = 0$ K – i.e. no atoms residing in antisite positions. In the first approximation, no effects connected with the tetragonal distortion in the $L1_0$-ordered structure were

taken into account. The resulting isothermal time evolutions of η were analysed by means of Laplace transformations.

3.2. Results of computer simulations

3.2.1. Bulk samples

Both for $L1_2$-ordered Ni_3Al and $L1_0$-ordered FePt the simulations showed discontinuous "order-disorder" transformations (complete disordering) at temperatures T_t close to the experimental data[2]. The $\eta(t)$ relaxations showed two time scales – i.e. the Laplace transforms of the curves showed exactly two peaks indicating two relaxation times τ_S and τ_l (Figs.3a, b).

[2] *For the case of Ni_3Al this means the temperature higher than the melting point and determined by means of extrapolation (for references see [1]).*

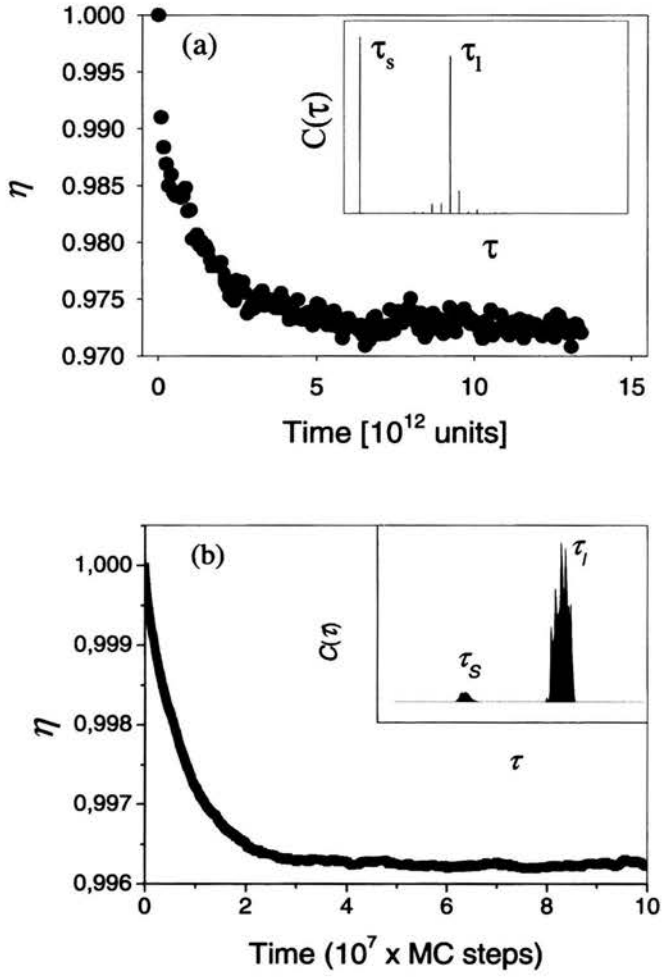

Fig.3. Examples of simulated η(t) relaxations in Ni_3Al [19] (a) and FePt [7] (b). Insertions show the corresponding Laplace transforms

The contribution of the fast relaxation component in FePt was, however, very small and the process decayed at higher temperatures. Both in Ni_3Al and FePt the presence or absence of the fast relaxation

component[3] was correlated with the character of the time evolution of *APC* (Figs. 4a,b), as well as with the relationship between frequencies of the atomic jumps leading to disordering (executed between sites belonging to different sublattices) and those executed within one sublattice by antisite atoms (Figs.5a-d).

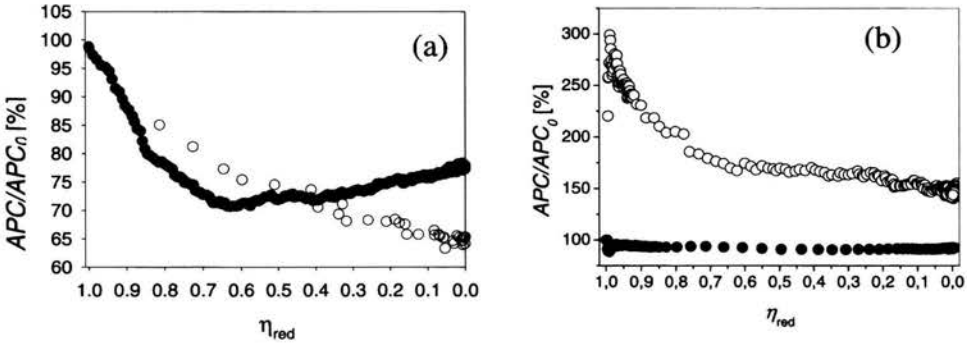

Fig.4. Isotherms of the SRO parameter APC normalised to the initial value APC_0 as a function of η_{red} in Ni_3Al (a) and FePt (b) : the case of two time scales (○) and the case of a single time scale (●). $\eta_{red} = (\eta-\eta_{eq})/(1-\eta_{eq})$, where η_{eq} denotes the equilibrium value of η

As follows from the graphs, in FePt these relationships were "inverted" with respect to those observed in Ni_3Al: while in $L1_2$-ordered Ni_3Al *the lack of the fast relaxation* component meant a fast decrease of *APC* (after its immediate increase up to the level of 1 meaning that disordering started by a formation of a pair of antisites) and $P_{Al:Ni\rightarrow Ni} > P_{Al:Al\rightarrow Ni}$ [18,19], in $L1_0$-ordered FePt, the fast decrease of *APC* (following its initial increase which, however, proceeded slower than in

[3] *In Ni_3Al the fast relaxation component might be eliminated by appropriately handling atomic pair-interaction energies [17,18].*

the case of Ni_3Al) and a high value of $P_{Pt:Fe\rightarrow Fe}$ (in relation to $P_{Pt:Pt\rightarrow Fe}$) was observed *in the presence* of the fast relaxation component.

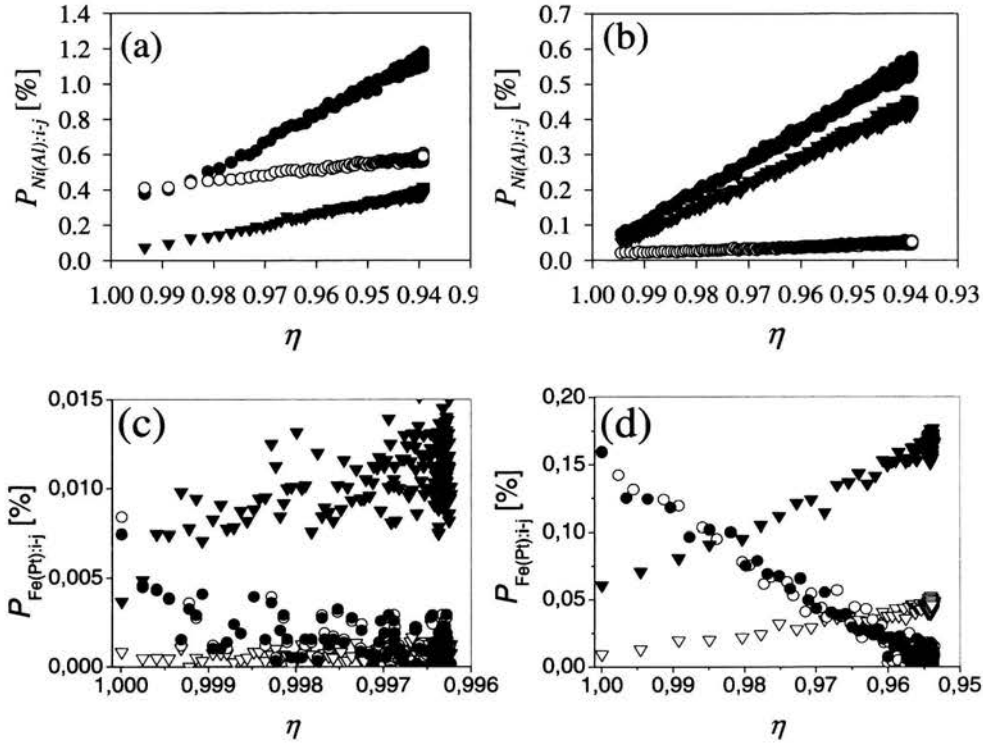

Fig.5. Isothermal atomic-jump statistics for the case of: two time scales in Ni_3Al (a) and a single time scale in Ni_3Al (b): $P_{Ni:Ni\rightarrow Al}$ (●), $P_{Al:Al\rightarrow Ni}$ (○) and $P_{Al:Ni\rightarrow Ni}$ (▼); two time scales in FePt (c) and a single time scale in FePt (d): ($P_{Pt:Pt\rightarrow Fe} - P_{Pt:Fe\rightarrow Pt}$) (●), ($P_{Fe:Fe\rightarrow Pt} - P_{Fe:Pt\rightarrow Fe}$) (○), $P_{Pt:Fe\rightarrow Fe}$ (▼) and $P_{Fe:Pt\rightarrow Pt}$ (▽). P denote jump frequencies (Eq.6)

3.2.2. Nano-layers

The reaction of the system on the removal of [001]-direction periodic boundary conditions – i.e. on the creation of two (001)-type free surfaces limiting the crystal, depended on the particular $L1_0$ superstructure variant.

In the samples $L1_0$-ordered in x-variant a gradual decrease of $L1_0$ stability showed up when the layer was thinned down to 10 atomic planes. Thinning below 20 atomic planes caused a considerable slowing-down of the "order-order" kinetics, however, the process still consisted of a homogeneous generation of antisite defects and, similarly as in the bulk, showed two time scales.

In the case of the z-variant of $L1_0$-order, totally different evolution of the atomic configuration was observed.

Fig.6 shows a projection of two subsequent (010)-type atomic planes of a layer composed of 80 (001)-type monoatomic planes (a bulk sample with removed [001] periodic boundary conditions) relaxed at 1200 K. As follows from the figure, the disordering process ran in two modes:

- homogeneous disordering – generation of antisites within the volume of the layer (as in the bulk),
- the formation of domains of x- and y- $L1_0$ variants: they nucleated at the Fe-surface and grew inwards the layer. The Pt surface was definitely stable, which apparently followed from the strong repulsion between Pt atoms, which "avoided" jumping to the antisite positions within the layer volume. This repulsion can be

attributed to the larger size of the platinum atoms that is in favour of their segregation towards the surface [22].

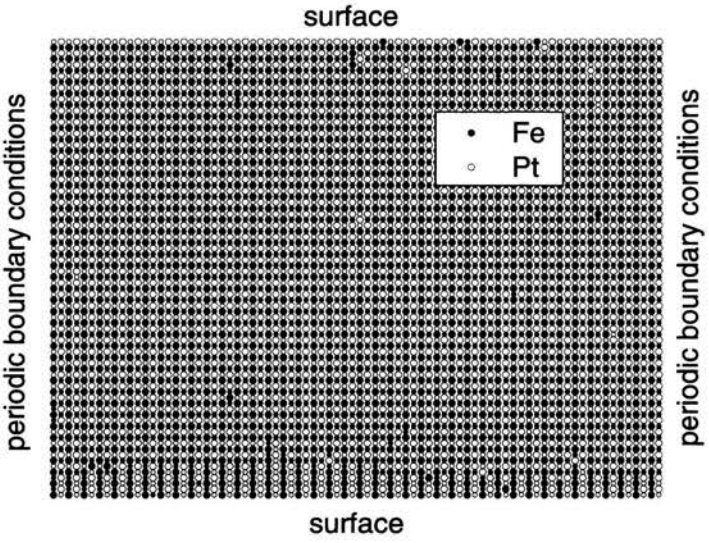

Fig. 6. Projection of n-th (larger circles) and (n+1)-th (smaller circles) (010)-type atomic planes in a z-variant $L1_0$-ordered FePt layer with d=80 after 5×10^7 MC Steps executed at T = 1200 K

The kinetics of the process could no longer be represented by the η parameter defined in Eq.(3) (numerotation of sublattices was no longer fixed), however, it was well represented by the time evolution of the NNCOR's (Eq.5).

The process running at 1200 K in a layer 10-planes thick, where the transformation completed within a reasonable CPU time, is illustrated by three "snap-shots" of the microstructure evolution (Fig.7).

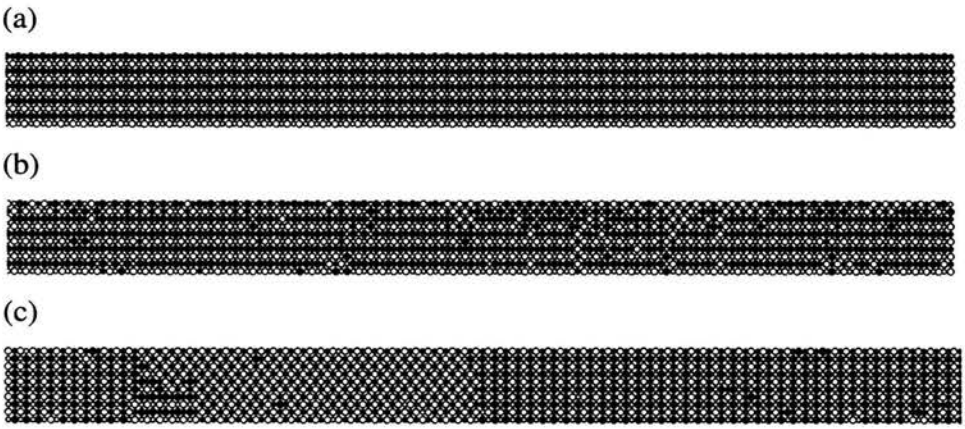

Fig.7. Projections of n-th (larger circles) and (n+1)-th (smaller circles) (010)-type atomic planes in a z-variant $L1_0$-ordered FePt layer with d=10: (a) initial atomic configuration; (b) atomic configuration after 10^7 MC Steps executed for T = 1200 K; (c) atomic configuration after 5×10^8 MC Steps executed at T = 1200 K

The detailed kinetics of the process is shown in Fig.8 as a MC-time dependence of NNCOR parameters. The following steps are observed :

- The Fe surface atoms enter the layer volume and occupy antisite positions; $NNCOR_{Fe}$ shows a first fast increase. As some Pt-atoms are replacing the Fe-atoms on the surface and transitorily loose their nn co-ordination with other Pt-atoms, a transient decrease of $NNCOR_{Pt}$ is observed.

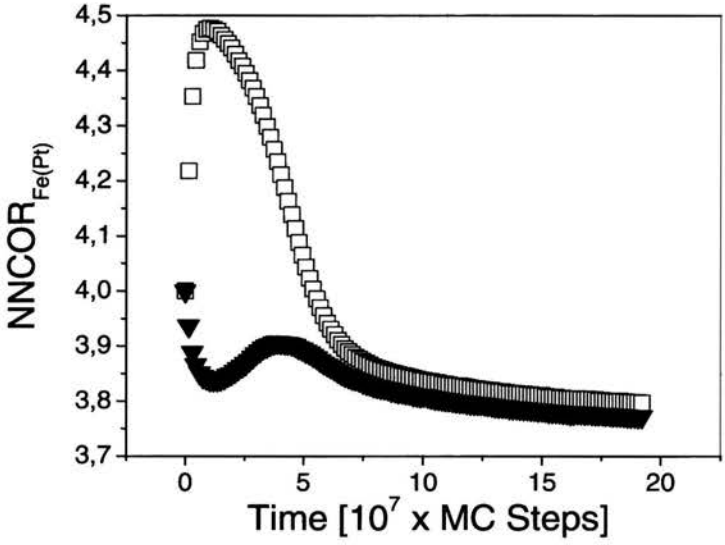

Fig. 8. $NNCOR_{Fe}(t)$ (□) and $NNCOR_{Pt}(t)$ (▼) isotherms in z-variant $L1_0$-ordered FePt layer with d=10 simulated at T=1200 K

- Subsequently, $NNCOR_{Pt}$ also increases, because of the decrease of the degree of LRO in the z- $L1_0$ variant (in the disordered phase, NNCOR = 6).
- Finally, both $NNCOR_{Fe}$ and $NNCOR_{Pt}$ decrease to a level lower than 4, which corresponds to the definite formation of the x- and y-variant $L1_0$ superstructure domains and illustrates the fact that all the monoatomic layers are cut by the surfaces in the $L1_0$ x- and y-variants (in contrary to the z-variant), which lowers the average value of $NNCOR_{Fe(Pt)}$ and apparently predominates the expected increase of $NNCOR_{Fe(Pt)}$ due to the formation of antiphase domains.

Temperature dependence of the kinetics of the process is shown in Fig.9.

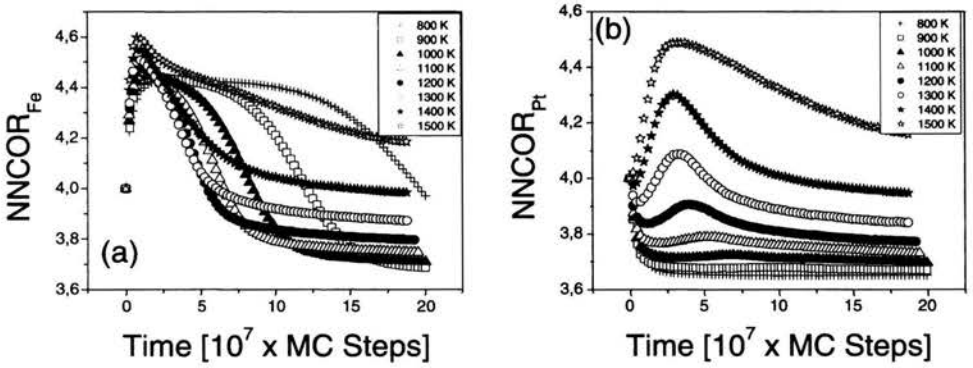

Fig. 9. (a): NNCOR$_{Fe}$(t) and (b): NNCOR$_{Pt}$(t) isotherms in z-variant L1$_0$-ordered FePt layer with d=10 simulated at marked temperatures

The best marked feature is the decay of the transient increase of NNCOR$_{Pt}$ at low temperatures accompanied by an enlargement of the plateau of NNCOR$_{Fe}$ (t). The initial fast increase of NNCOR$_{Fe}$ and simultaneous decrease of NNCOR$_{Pt}$ follow from the ordering of atoms on the (initially) Fe-surface. The x- and y-variant domains grow plane-by-plane by advancing the antiphase boundaries and without creating any additional antisites. The final decrease of NNCOR$_{Fe}$ starts when the domains percolate the layer as only then the effective area of the antiphase boundaries (where the Fe-Fe nn co-ordination is high) reduces. An increase of temperature means more chaotic transition between the L1$_0$ variants and the overall reduction of the degree of LRO. This acts towards an increase of both NNCOR$_{Fe}$ and NNCOR$_{Pt}$ and at sufficiently high temperatures predominates the above explained decreasing tendency

of $NNCOR_{Pt}$. Final formation of well formed x- and y-variant domains always leads to a decrease of the NNCOR's.

4. Discussion

4.1. General remarks

The presented results show the variety of features characterising "order-order" kinetics in stoichiometric binary intermetallic phases with different types of superstructures. The crucial importance of the superstructure geometry on the atomistic mechanism of "order-order" relaxations is revealed.

The examined systems fall into two main categories:

- B2-type ordered "triple-defect" AB compounds represented by NiAl:

  The fact that only A-B bonds build the first co-ordination shell in this superstructure results in a high antisite formation energy often comparable or higher than the corresponding vacancy formation energy (see e.g. [23]). As a result, the system disorders by generating "triple defects", which on the one hand means a very high vacancy concentration, but on the other hand "immobilisation" of triple-defect vacancies, which no longer take part in the creation of further antisites [15]. Consequently, "order-order" relaxations in such systems are sluggish, though showing moderate activation energies (Fig.2a).

- $L1_2$- and $L1_0$-type ordered A_3B and AB compounds.
  Because of mixed 1st-shell co-ordination, the vacancy formation energy is usually higher than that for antisite formation (see e.g. [24]). Consequently, the $L1_2$- and $L1_0$-ordered intermetallics show very low vacancy concentration [16]. However, the existing vacancies are all active as atomic-jump agents and antisites may continuously be created without an increase of vacancy concentration. As a result, the "order-order" relaxations proceed faster than they do in "triple-defect" systems.

4.2. Activation energies for "order-order" relaxation and self-diffusion

The relationship between the activation energies $E_A^{(O-O)}$ for "order-order" relaxations and the ones $E_A^{(D)}$ for self-diffusion of the components are also specific for particular superstructure geometries. The case of the "triple-defect" NiAl was discussed in the previous paper [15] in terms of the differences between atomistic mechanisms of "triple-defect" diffusion and "triple-defect" ordering.

In contrast to the B2-type superstructure, atoms may migrate in the $L1_2$- and $L1_0$-type structures by jumping to nn vacancies without disturbing the state of chemical order. The properties of these "easy" diffusion channels determine the relationship between $E_A^{(O-O)}$ and $E_A^{(D)}$. While in the case of $L1_2$ easy diffusion may proceed within the majority sublattice (75 % of all lattice sites), easy migration in $L1_0$ is possible along the monoatomic planes. However, the capacity of these channels is

substantially lower (with respect to the majority sublattice in $L1_2$) and thus, self diffusion may involve also interplanar jumps, which would reduce (and perhaps even invert with respect to $L1_2$) the difference between $E_A^{(O-O)}$ and $E_A^{(D)}$ - as observed in the case of FePd. Another explanation of the inverted relationship between $E_A^{(O-O)}$ and $E_A^{(D)}$ in $L1_2$ and $L1_0$ superstructures might be given in terms of the degree of atomic jump correlation during diffusion and "order-order" relaxation: Recent Molecular Dynamics studies [25] showed that high correlation of atomic jumps may result in an increase of the effective activation energy of related processes evaluated from appropriate Arrhenius plots. While in the case of the $L1_2$ superstructure ordering/disordering requires definitely higher atomic-jump correlation than does diffusion, it is just diffusion, which requires more atomic-jump correlation in the $L1_0$ case.

The relatively low average value for $E_A^{(O-O)}$ in FePd resulting from "in situ" experiments [7] is in agreement with the migration enthalpy $H_M \approx 0.9$ eV evaluated for this compound on the basis of inelastic neutron scattering [26]. However, the REST-obtained value of $E_A^{(O-O)} = (2.7 \pm 0.1)$ eV reported in ref. [6] is quite close to the "in situ"-obtained $E_A^{(O-O)} = (2.3 \pm 0.2)$ eV related to the slow relaxation component at temperatures below the Curie point [7].

Finally, the preliminary result obtained for FePt ($E_A^{(O-O)} = 0{,}8$ eV) is close to the activation energy $E_A = 0.74$ eV for $L1_0$-ordering in FePt thin film measured by high-temperature X-ray diffraction [27].

4.3. Two time scales in "order-order" relaxations.

The origin of the coexistence of two time scales observed in the "order-order" relaxations in Ni_3Al, FePd and FePt was revealed by means of kinetic MC simulations.

The mechanism of the effect in Ni_3Al has been explained in detail in our previous paper [18] and the validity of the proposed model has recently been confirmed for the case of other $L1_2$-ordered A_3B binaries [28].

The model is illustrated by a scheme in Fig. 10 showing a sequence of two correlated jumps of B- and A-atoms creating a pair of nn antisites (Fig.10a). Such a process is very effective in decreasing the degree η of LRO and shows up as the fast relaxation component. It saturates, however, before η has reached its equilibrium value. The continuation of the relaxation, constituting the slow relaxation component, is possible due to B-antisite "easy" diffusion within the A-sublattice, which leads to uncoupling the nn antisite pairs and enabling their further generation (Fig.10b). As shown in ref. [18], the origin of two time scales in *ordering* relaxations can be explained in the same terms.

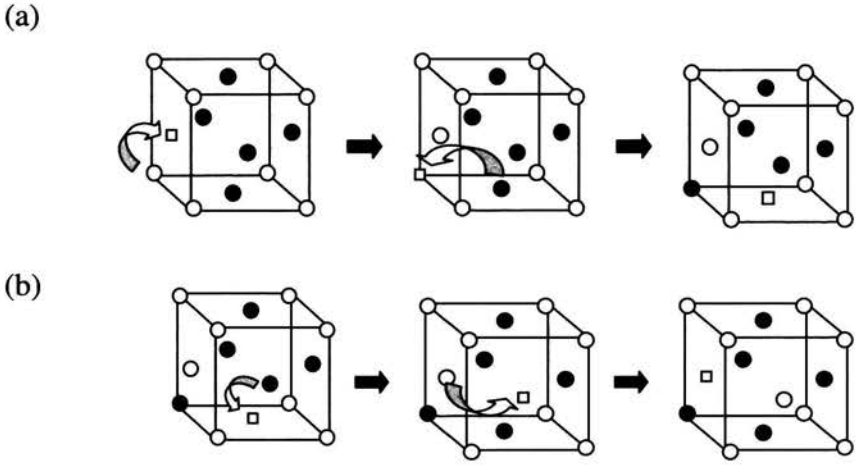

Fig.10. Sequences of correlated atomic jumps in Ni_3Al leading to (a): a generation of a nn pair of Ni- and Al-antisites and (b): uncoupling of such a pair. ○ – Al atoms, ● - Ni atoms

The MC simulations have recently been extended to AB binaries ordered in $L1_0$ superstructure. The scheme presented in section 3.1 has been applied first to a prototype system [28] and most recently to stoichiometric FePt intermetallic. Only $T_i = 0$ K $\rightarrow T_f$ disordering relaxations have up to now been simulated systematically. As shown in ref.[28] and in section 3.2, the situation is less clear than in $L1_2$-ordered A_3B systems. The "time-scale" structure of the relaxations seems to be considerably dependent on the particular energetics of the compound. However, the "multi-time-scale" character of the relaxations has been definitely confirmed, although one process always predominates with about 90 % contribution to the entire relaxation. Despite these difficulties, the results presented in section 3.2 enable us to propose a model, which stresses the definite effect of specific superlattice geometry

and in particular, the geometry of "easy diffusion channels" on the features of "order-order" relaxations.

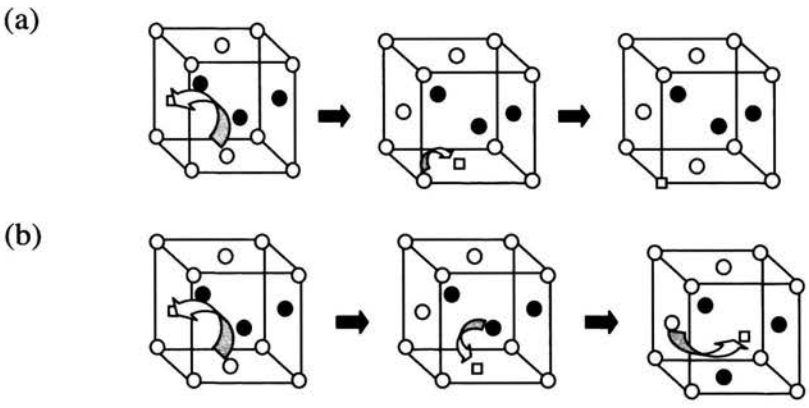

Fig.11. Sequences of correlated atomic jumps in FePt leading to (a): a generation of a single Pt-antisite and (b): a generation of a nn pair of Pt- and Fe-antisites. ○ *– Pt atoms,* ● *- Fe atoms*

It should first be noted that, in contrary to $L1_2$ superstructure, easy diffusion is possible in the $L1_0$ within both A- and B-sublattices. It is, therefore, possible that single antisite defects are generated (after *any* single disordering jump the vacancy may "escape" without returning to the initial sublattice, as it is the case in $L1_2$ geometry) (Fig. 11a). Generation of nn antisite pairs, i.e. fast decrease of η (fast relaxation component), is also possible (Fig. 11b), but such events are less probable. If a nn antisite pair is produced (initial increase of *APC*, Fig. 4b), the active vacancy is finally back on the initial sublattice and may "serve" as a migration agent for the antisite, which was first generated. Such a model would explain the observed correlation between the existence of the fast relaxation component and the increase of the frequency of Pt-

antisite diffusion jumps with respect to the "disordering" jumps (Fig. 5c). The "easy" diffusion of Pt-antisites means, of course, uncoupling of the generated nn antisite pairs, which is reflected in a fast decrease of *APC* in the corresponding relaxations (Fig. 4b).

Taking into account the low probability of the jump sequences leading to the above mechanism, one may understand that the process decays at higher temperatures, where entropy becomes more important in controlling the relaxation. Detailed simulation studies of "order-order" relaxations in $L1_0$-ordered binaries, including reversible ordering and disordering processes are in progress.

4.4. Structural transformations in FePt thin layers

The presented first results of the MC simulations of "order-order" phenomena in FePt nano-layers showed a strong effect of free surfaces on the process. The crucial result is an indication of the definite preference imposed by the Fe-surface on the longitudinal (x- and y-) $L1_0$-superstructure variants and of the stabilization effect of Pt-surface on the perpendicular (z-) superstructure variant. Although, as follows from the experimental studies (see e.g. [30-32]), the conditions of thin-film deposition including the substrate type and orientation are the crucial factors controlling the $L1_0$-film orientation (texture), the thermodynamic properties of the film itself are of great importance. The definitely higher stability of the $L1_0$ variant with c-axis parallel to the FePt film surface seems worth considering when designing longitudinal magnetic

recording media on the basis of this intermetallic compound. Possible technology should apparently base on the deposition and subsequent annealing of an FePt film limited by the Fe monoatomic layer.

Conclusions

- Extensive resistometric investigation of "order-order" kinetics in binary intermetallics with $L1_2$-, $L1_0$- and B2-type superstructures indicate a definite correlation between "order-order" relaxations and superstructure geometry. The experimental results on $L1_2$-ordered Ni_3Al and $L1_0$-ordered FePt appear partially explainable by means of kinetic Monte Carlo simulation of the process.
- Different relationships between activation energies for tracer diffusion and for "order-order" kinetics in Ni_3Al and FePd (FePt) may follow from different relationships between atomic-jump correlation during ordering/disordering and diffusion in these systems. The above relationships, in turn, follow from the capacities of "easy-diffusion" channels available in both fcc-based superstructures.
- Multi-time-scale character of the "order-order" relaxations in $L1_2$- and $L1_0$-ordered binaries follows in both cases from a specific interplay between long-range (antisite formation) and short-range ordering (generation of nn antisite pairs). However, due to differences in stoichiometries and geometries, the processes in

both superstructure-types are different: the short-range ordering component shows a much lower profile in $L1_0$ ordered systems.

- It is postulated that the triple-defect mechanism of ordering in B2-ordered NiAl is responsible for the observed low rate of relaxations despite high vacancy concentration.
- Monte Carlo simulations of "order-order" kinetics in FePt nano-films indicated an important effect of surfaces on the atomistic mechanism of the process and reproduced the phenomenon of spontaneous $L1_0$-superstructure reorientation leading to "perpendicular magnetic anisotropy".

Acknowledgements

The work was partially supported by the Austrian Government: bm:bwk (GZ 45.529/2-VI/B/7a/2002).

References

1. R. Kozubski: Prog. Mater. Sci. 41 (1997) 1.
2. S.V. Divinski, St. Frank, Chr. Herzig, U. Södervall: Solid State Phenomena 72 (2000) 203.
3. H. Numakura, T. Ikeda, M. Koiwa, A. Almazouzi: Philos. Mag.A. 77 (1998) 887.
4. R. Kozubski, M. C. Cadeville: J. Phys. F. : Met. Phys. 18 (1988) 2569.
5. H. Yamauchi, D. de Fontaine in: H. Warlimont (Ed.) Order-disorder transformations in alloys, Springer, Berlin (1974) 148.
6. A. Kulovits, W.A. Soffa, W. Püschl, W. Pfeiler: Mater. Res. Soc. Symp. Proc. 753 (2003) BB5.37.1.

7. R. Kozubski, M. Kozłowski, V. Pierron-Bohnes, W. Pfeiler, Z.Metallkde. 95 (2004) 10.
8. B. Sitaud, X. Zhang, C. Dimitrov, O.Dimitrov in: H.E.Exner, V.Schuhmacher (Eds.) Advanced Materials and Processes, DGM, Oberursel (1990) 389.
9. R. Kozubski, J. Sołtys, M. C. Cadeville: J. Phys.: Condensed Matter. 2 (1990) 3451.
10. St. Frank, U. Södervall, Chr. Herzig: Phys. Stat. Sol. b191 (1995) 45.
11. J. Fillon, D. Calais: J. Phys. Chem. Solids 38 (1977) 81.
12. J. Kučera, B. Million: phys.stat.sol. (a) 31 (1975) 275.
13. Y. Nose, T. Ikeda, H. Nakajima, K. Tanaka, H. Numakura, Mater. Res. Soc. Symp. Proc. 753 (2003) BB5.36.1.
14. H. Lang, K. Rohrhofer, P. Rosenkranz, R. Kozubski, W. Püschl, W. Pfeiler: Intermetallics 10 (2002) 283.
15. R. Kozubski, D. Kmieć, E. Partyka, M. Danielewski: Intermetallics 11 (2003) 897.
16. H.-E. Schaefer, K. Frenner, R. Würschum: Intermetallics 7 (1999) 277.
17. St. Frank, S.V. Divinski, U. Södervall, Chr. Herzig: Acta Mater. 49 (2001) 1399.
18. P. Oramus, R. Kozubski, V.Pierron-Bohnes, M.C.Cadeville, W.Pfeiler: Phys. Rev. B 63 (2001) 174109.
19. P. Oramus, R. Kozubski, V.Pierron-Bohnes, M.C.Cadeville, C.Massobrio, W.Pfeiler: Mater. Sci. Eng. A 324 (2002) 11.
20. M. Kozłowski, R. Kozubski, V. Pierron-Bohnes, W. Pfeiler, Comput.Mater.Sci. – in press
21. T. Mohri, C. Ying: Mater. Trans. 43 (2002) 2104.
22. Y. Gauthier, Surf.Rev.Letters, 3 (1996) 1663.
23. B. Meyer, M. Faehnle: Phys. Rev. B59 (1999) 6072.
24. H. Schweiger, O. Semenova, W. Wolf, W. Pueschl, W. Pfeiler, R. Podloucky, H. Ipser: Scripta Mater. 46 (2002) 37.
25. P. Oramus, C. Massobrio, M. Kozłowski, R. Kozubski, V. Pierron-Bohnes, M. C. Cadeville, W. Pfeiler: Comput. Mater. Sci. 27 (2003) 186.
26. T. Mehaddene, E. Kentzinger, B. Hennion, K. Tanaka, H. Numakura, A. Marty, V. Parasote, M.C. Cadeville, M. Zemirli, V. Pierron-Bohnes: Phys. Rev. B69 (2004) 024304.

27. F. E. Spada, F. T. Parker, C. L. Platt, J. K. Howard: J. Appl. Phys. 94 (2003) 5123.
28. P. Oramus, M. Kozłowski, R. Kozubski. V. Pierron-Bohnes, M. C. Cadeville, W. Pfeiler: Mater. Sci. Eng. A 365 (2004) 165.
29. T.B. Massalski: Binary Alloy Phase Diagrams. ASME, Metals Park, OH, 1987.
30. M.M. Schwickert, K.A. Hannibal, M.F. Toney, M. Best, L. Folks, J.-U. Thiele, A.J. Kellock, D. Weller: J.Appl.Phys., 87 (2000) 6956.
31. M-G. Kim, S-C. Shin: J.Appl.Phys., 90 (2001) 2211.
32. T. Mahalingam, J.P. Chu, J.H. Chen, C.L. Chiang, S.F. Wang, Mater.Chem.Phys. 82 (2003) 335.